Geotech Geol Eng (2024) 42:3251–3267
https://doi.org/10.1007/s10706-023-02727-8

ORIGINAL PAPER

Numerical Study of Consolidation of Slurry Tailings Considering Continuous Update of Material Properties

Ngoc Dung Nguyen · Thomas Pabst

Received: 9 September 2023 / Accepted: 6 December 2023 / Published online: 2 February 2024
© The Author(s) 2024

Abstract Explicitly modelling tailings consolidation behaviour contributes to improve integrated management approaches and accurately estimate the storage capacity of tailings storage facilities (TSFs) to better predict their static and dynamic stability. However, slurry tailings demonstrate a highly non-linear evolution of stiffness and hydraulic conductivity during consolidation, thus significantly complexifying the determination of their hydromechanical properties. In this study, an approach to update Mohr Coulomb parameters and simulate the continuous evolution of hydraulic conductivity and stiffness of tailings materials with the reduction of the void ratio was proposed and embedded in a finite difference code to more realistically simulate the evolution of material properties during sequential loadings. The model was validated using laboratory column tests and various predictive functions were tested to estimate hydraulic conductivity for field applications. Finally, the developed approach was applied to a simplified model of tailings impoundment to illustrate practical applications. Results from this study indicated that the approach developed was able to capture the non-linearity properties of tailings during consolidation, and that using continuously updated stiffness and hydraulic conductivity could induce significantly different magnitude and rate of consolidation than models with constant properties. Predictive models such as Kozeny–Carman and Kozeny–Carman Modified models also gave a satisfactory estimation of tailings behaviour, at least for preliminary studies. The simple modifications to the numerical codes proposed in this paper could therefore significantly improve the numerical simulation of tailings behaviour in the short term and contribute to a better planning of deposition plans.

Keywords Slurry tailings · Consolidation · Updated properties · Predictive equation · Coupled numerical simulation

Supplementary Information The online version contains supplementary material available at https://doi.org/10.1007/s10706-023-02727-8.

N. D. Nguyen · T. Pabst (✉)
Department of Civil, Geological and Mining Engineering, Polytechnique Montreal, Montreal, QC H3C 3A7, Canada
e-mail: thomas.pabst@ngi.no

N. D. Nguyen · T. Pabst
Research Institute on Mines and Environment (RIME UQAT-Polytechnique), Montreal, Canada

N. D. Nguyen
Department of Geo-Engineering and Geotechnic, Hanoi University of Mining and Geology, Hanoi 100000, Vietnam

T. Pabst
Norwegian Geotechnical Institute (NGI), Oslo, Norway

1 Introduction

Hard rock mine tailings generated during mining operations are typically deposited as slurry in tailings storage facilities (TSFs) and consolidate with time (Townsend and McVay 1990). Consolidation of mine tailings in TSFs can take a very long time because of their initially high-water content and their relatively low hydraulic conductivity (Azam et al. 2014; Da Silva et al. 2021). Consequently, tailings mechanical properties remain somewhat poor and expose TSF to various geo-environmental and geotechnical instabilities (e.g., dam failures and dynamic and/or static liquefaction) with significant risks for mining activities as well as the surrounding environment (Azam and Li 2010; Rana et al. 2021; Fourie et al. 2022). Special management methods, therefore, might be required to improve the hydro-mechanical properties of tailings (James and Aubertin 2017; Chai et al. 2023). Moreover, estimating the volume of tailings that can be stored in the TSFs in the short and long term also remains challenging.

Conventional estimation of consolidation of geomaterials is usually based on Terzaghi's consolidation theory with the principal assumption that hydraulic conductivity and the coefficient of compressibility are constant over time, while, in practice, hydraulic conductivity and compressibility vary with void ratio (Somogyi 1980; Schiffman 1982; Morris 2002). A general form of one-dimensional non-linear finite strain consolidation for saturated thick soil layers was therefore proposed by Gibson et al. (1967) to overcome the limitations of the small strain theory. Gibson's equation can accommodate large strain evolution and variations in hydraulic conductivity and stiffness during consolidation and is, therefore, more representative of tailings behaviour in field conditions (Schiffman 1982; Ahmed et al. 2023; Gheisari et al. 2023; Islam et al. 2023). Assuming constant properties for slurry tailings may be easier, but can also have significant implications, sometimes leading to an underestimation of the real consolidation time by several years (McDonald and Lane 2010). Considering changes in stiffness and hydraulic conductivity of tailings seems, therefore, necessary to improve the understanding of the short-term behaviour of tailings.

Various mathematical functions representing the relationship between effective stress and void ratio for tailings materials have been proposed (Table 1), including power function (Somogyi 1980), extended power function (Liu and Znidarčić 1991), logarithmic function (Bartholomeeusen et al. 2002), and Weibull function (Jeeravipoolvarn et al. 2008). Each function has its own advantages and limitations. For example, the extended power function proposed by Liu and Znidarčić (1991) can define the void ratio at zero effective stress, while power function cannot. Weibull function is particularly adapted to capture the preconsolidation behavior of oil sand tailings under loadings (Jeeravipoolvarn et al. 2008), but is more rarely used for hard rock mine tailings. The power function is often used for its simplicity and good representativeness (Townsend and McVay 1990; Agapito and Bareither 2018; Zhou et al. 2019). Best practice usually consists of choosing the most adequate function (and in determining its parameters) using experimental tests (Jeeravipoolvarn et al. 2008).

A power function is also commonly used to estimate the variation of hydraulic conductivity as a function of the void ratio for slurry materials (Somogyi 1980; Fredlund et al. 2015):

$$k = Ge^{H} \tag{1}$$

Table 1 Most common formulation of relationship between void ratio and effective stress (with e: void ratio; $\sigma\prime$: effective stress (kPa); A, B, C, D, E, and F are empirical adjustment parameters determined by experimental tests

Equations	Functions	Authors
$e = A\sigma^{'}B$	Power function	Somogyi (1980)
$e = A(\sigma^{'} + B)^{C}$	Extended power function	Liu and Znidarčić (1991)
$e = Aln\sigma^{'} + B$ $e = C\ln(k) + D$	Logarithmic function	Bartholomeeusen et al. (2002)
$e = A - B\exp[-E.\sigma^{'F}]$	Weibull function	Jeeravipoolvarn et al. (2008)

where k is the hydraulic conductivity (m/s), and G and H are also empirical adjustment parameters. This equation is rather simple to apply but must be calibrated against measurements of hydraulic conductivity for various void ratios, which can be time consuming.

Numerical models are then usually performed for upscaling laboratory results to field conditions. However, these studies were carried out with the assumption that either the tailings properties were constant (McDonald and Lane 2010) or they were updated after the addition of each new tailings layer (Boudrias 2018). Using continuously updated values of hydraulic conductivity and stiffness in future works was recommended by these studies to improve the estimation of consolidation of tailings. Zhou et al. (2019) validated the capability of explicit finite difference code FLAC (Itasca 2021) to consider non-linear evolution of tailings stiffness and hydraulic conductivity by modelling consolidation of clayey tailings under several disposition scenarios using continuously updated values of hydraulic conductivity and stiffness. However, these models were only in 2D analysis, and how to implement this method in the code was not detailed. Models with 3D analysis might be required in cases where the complexity of TSFs geometry and drainage boundary/configurations are encountered (Fredlund et al. 2015; Nguyen and Pabst 2023a, b).

The objective of this research was, therefore, to perform a series of coupled fluid-mechanical simulations using FLAC3D (Itasca 2021) to evaluate the potential differences between models using constant and continuously updated parameters. An approach to modify Mohr Coulomb parameters was first developed and integrated into FLAC3D, and it was then validated using laboratory column test results. To facilitate the application of this approach in other studies, a modelling flow chart and the FISH code are provided in Fig. 4 and in the Supplementary materials section, respectively. A parametric analysis evaluating the effect of various estimation methods of the hydraulic conductivity on porewater pressure (PWP) dissipation rate was also performed. Finally, the model was evaluated at a larger scale by simulating a simplified tailings impoundment inspired by a real case study.

2 Material Properties and Methodology

2.1 Tailings Samplings and Characterization

Tailings were sampled from the concentrator of a partner gold mine site in Quebec, Canada, and transported to the laboratory at Polytechnique Montreal for characterization. Tailings particles size distribution (PSD) was determined using ASTM D7928-17 (2017) for particles finer than 75 µm and ASTM D6913-17 (2017) for coarser particles. The value of D_{10} (the diameter corresponding to 10% passing in the particle-size distribution curve) was 0.004 mm, D_{60} (the diameter corresponding to 60% passing in the particle-size distribution curve) was 0.04 mm, and the coefficient of uniformity C_u ($C_u = D_{60}/D_{10}$) was 10 (Fig. 1). These hard rock mine tailings were classified as low plasticity silts (ML) according to the Unified Soil Classification System (ASTM D2487-17 2017). The specific gravity was 2.75 in this study (Essayad and Aubertin 2021). Modified proctor test was performed according to ASTM D1557-12 (2012) which indicated an optimum moisture content $W_{opt} = 13\%$ and a maximum dry density, γ_{dmax} = 1830 kg/m^3. These properties were typical of hard rock mine tailings (Qiu and Sego 2001; Bussière 2007). A friction angle of 38 degrees was applied and tailings were considered cohesionless (Boudrias 2018). Initial porosity of tailings was 0.437, and a value of 0.28 (calculated based on friction angle as $\nu = \frac{1-sin\theta'}{2-sin\theta'}$) (Holtz and Kovacs 1981) was used for Poisson's ratio.

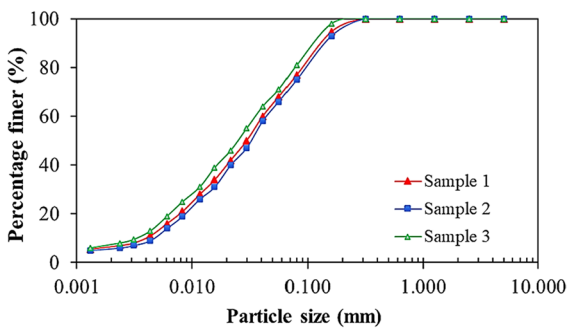

Fig. 1 Particle size distribution of Malartic tailings used in this study

2.2 Consolidation Tests

Conventional oedometer tests are widely used to evaluate the compressible properties of soils using the small strain Terzaghi's theory (Holtz and Kovacs 1981). However, oedometer tests are not adapted to slurry materials (such as tailings and dredged soils) because of their initially low density and high-water content (Ahmed and Siddiqua 2014; Tian et al. 2019; Ahmed et al. 2023). For example, the compressibility of tailings slurry at very low pressure (i.e., less than a few kPa) is critical (Tian et al. 2019), but the initial loading pressure in the oedometer test is usually 5 kPa (Holtz and Kovacs 1981). Thus, conventional oedometer test does not cover the non-linear behavior of tailings. Finally, the constitutive relations between void ratio and effective stress and void ratio and hydraulic conductivity are essential for the estimation and simulation of consolidation of tailings, which cannot be obtained from the oedometer test (Ahmed and Siddiqua 2014; Ngo et al. 2020; Ahmed et al. 2023). Column consolidation tests were therefore proposed by Essayad and Aubertin (2021) to overcome such limitations. Tailings are poured into instrumented columns to investigate consolidation behaviours of tailings under incremental loadings with the continuous monitoring of excess pore water pressure at various elevations of the column (Essayad and Aubertin 2021).

In the present study, two such consolidation tests were performed, namely columns S1 and S2. Around 30 cm of slurry tailings were placed in 50 cm high and 10 cm internal diameter columns and compressed under incremental loadings (Fig. 2). Samples were prepared with a solid content of around 74% to prevent segregation during test setup (Essayad 2015; Boudrias 2018). Excess PWP was monitored continuously using three pore water pressure sensors (*Trustability*, precision: ±0.20%) installed 3.5 cm, 15 cm, and 23.5 cm from the base of the columns. A LVDT was placed on top of each column to measure the displacement at the surface of the tailings. Maximum excess PWP measured during the tests was up to 40% smaller than the loading applied at each step, which might be explained by the influence of side friction between tailings and instrumented columns wall or by the formation of tailings aggregate which could also share a portion of the external loading (Fig. 2). The effect of friction between the column wall and tailings was therefore corrected for both column tests at each loading step using the procedure proposed by Essayad and Aubertin (2021). Corrected values were used and presented in Table 2 (Nguyen 2022). Next loading step was applied when PWP reached hydrostatic equilibrium (Lévesque 2019; Essayad and Aubertin 2021). The maximum loading applied to the tailings in this study was around 200 kPa (corresponding to an overburden thickness of around 20 m), but larger values could be applied as well to reflect higher values of loading that might be encountered in the field.

In addition, saturated hydraulic conductivity was measured at the end of each loading stage for column S1 using constant head test inspired by ASTM D5856 (2015). A constant hydraulic head was applied at the

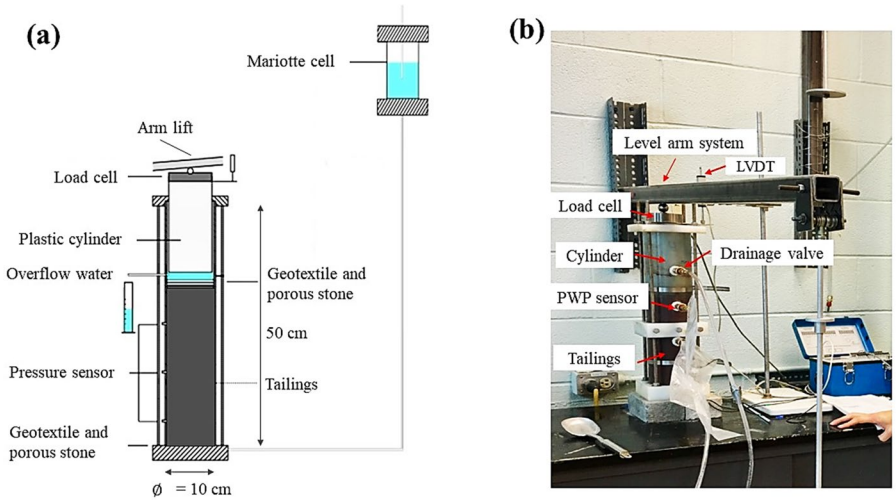

Fig. 2 Instrumented column test setup used to measure saturated tailings compressibility. A lever arm was used to apply increasing loading and a PVC cylinder transmitted the vertical compression loading to the tailings surface. LVDT and PWP sensors (placed at different elevations) were connected to a data logger (modified after Lévesque (2019) and Nguyen and Pabst (2020))

Table 2 Loading applied at various steps in column test S1 and S2 (values of loading was corrected for friction)

Loading steps	Column S1 (kPa)	Column S2 (kPa)
1	3.2	3.2
2	26.3	22.6
3	55.5	51.2
4	80.4	71.2
5	95.9	87.4
6	116.2	102.3
7	139.1	126.1
8	158.1	147.4
9	178.8	163.9
10	198.5	180.7

base of the column using a Mariotte cell (Fig. 2), and the outflow was measured at the upper drainage valve (Lévesque 2019). For practical reasons, the hydraulic conductivity was measured by imposing an upward flow, contrary to what is recommended by standard ASTM D5856 (2015), and results could, therefore, have been slightly underestimated.

2.3 Numerical Simulations

2.3.1 Conceptual Model

Column tests S1 and S2 were simulated in FLAC3D (Itasca 2021) as cylinders with a radius of 10 cm and a height of 30 cm. The cylinder walls were modeled as rigid boundaries where only vertical displacement was allowed. The mesh was vertically divided into 15 zones (mesh sensitivity analysis showed that finer mesh size had no significant influence on the rate of dissipation of PWP) (Nguyen 2022). PWP at tailings surface was fixed at zero to simulate the water table position and allow an upward free drainage condition (Bolduc and Aubertin 2014; Ferdosi et al. 2015; Mbemba and Aubertin 2021a). The bottom boundary was considered impervious similarly to laboratory conditions. Bottom boundary was fixed in all three directions. Loading was simulated at the surface of the model in 10 stages. Tailings properties were considered homogenous, which was deemed realistic even though void ratio may be different between the top and bottom of the column.

2.3.2 Hydraulic Conductivity and Stiffness Update

In this study, tailings stiffness and hydraulic conductivity were continuously updated to consider the effect of the variation of void ratio during consolidation. Void ratio was calculated from measured height (H) after each loading and heigh of solid (H_s) during the test ($e = \frac{H-H_s}{H_s}$), and a relation between void ratio and effective stress was established (Fig. 3a) ($R^2 = 0.97$):

$$e = 0.814 \times \sigma'^{-0.058} \tag{2}$$

Hydraulic conductivity decreased as void ratio decreased. For example, hydraulic conductivity at the end of cycle 3 was around 2 times smaller compared to that at the end of cycle 2 (Fig. 3b). A power law function of hydraulic conductivity was fitted on the experimental results ($R^2 = 0.99$):

$$k = 1.24 \times 10^{-6} e^{4.61} \tag{3}$$

Young's modulus was also calculated at each loading step based on Poisson's ratio (υ) and volumetric compressibility coefficient, m_v, that derived from the settlement curve at each load step ($E = \frac{(1+\upsilon)(1-2\upsilon)}{(1-\upsilon)m_v}$) (Holtz and Kovacs 1981). Tailings stiffness increased during each loading step and was for example almost three times greater at the end of cycle 2 compared to the load cycle 1 (Fig. 3c). The relation between Young's modulus and effective stress was then derived and fitted using the following power law function ($R^2 = 0.95$):

$$E = 85.6 \times \sigma^{0.74} \tag{4}$$

The extrapolation of the power function tended to lead to very small (and unrealistic) stiffnesses at small effective stresses (i.e., < 0.1 kPa), and a minimum value of the Young's modulus E = 180 kPa (corresponding to the Young's modulus of tailings at the first loading stage obtained from column tests) was therefore assigned in the models to prevent excessive displacements during the first loading step. Equations 2, 3 and 4 were introduced in the simulations via FISH coding language in FLAC3D to automatically update the hydraulic conductivity and stiffness values at each iteration. Initial height and loadings were adjusted based on column characteristics, but

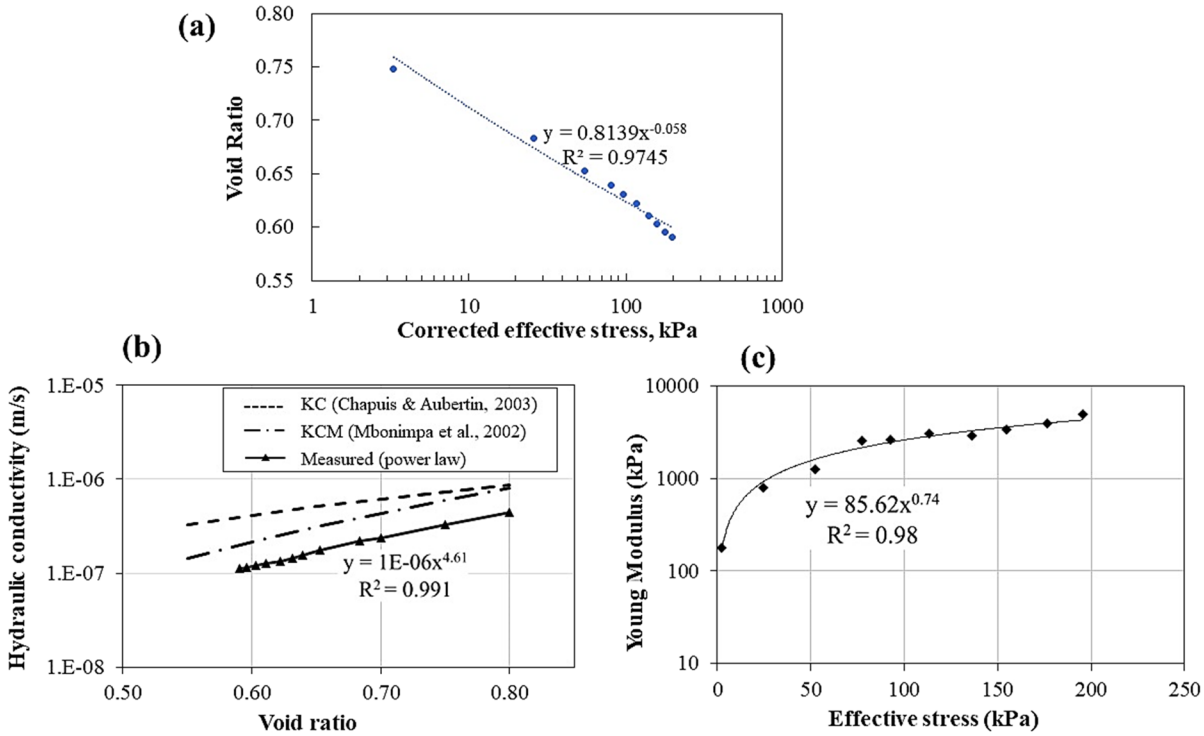

Fig. 3 Evolutions of **a** void ratio as a function of effective stress, **b** hydraulic conductivity as a function of the void ratio for and **c** Young's modulus as a function of effective stress for column test S1. Measurements (points) and fitted power law functions (solid lines) are shown. Experimental hydraulic conductivities are compared with KC (Chapuis and Aubertin 2003) and KCM (Mbonimpa et al. 2002) predictive models. It is noted that these functions were derived from results for column S1 and was considered identical for column S2 as the same materials were used for these 2 column tests

all the other parameters (i.e., density, Poisson's ratio and internal friction angle, and stiffness and hydraulic conductivity functions) were identical in both models.

2.3.3 Predictive Functions of Hydraulic Conductivity

In practice, measuring hydraulic conductivity can be time-consuming, especially if the measurements need to be repeated for several void ratios (Mbonimpa et al. 2002; Babaoglu and Simms 2020). Various predictive functions have, therefore, been proposed to estimate hydraulic conductivity from more common and easy-to-obtain parameters, such as the particle size distribution curve or limit of plasticity (Mbonimpa et al. 2002). KCM (Mbonimpa et al. 2002) model is based on Kozeny–Carman model (Chapuis and Aubertin 2003) and considers the tortuosity, the pore size distribution and the solid grain surface characteristics (Mbonimpa et al. 2002):

$$k_G = C_G \frac{\gamma_w}{\mu_w} \frac{e^{3+x}}{1+e} C_U^{1/3} D_{10}^2 \tag{5}$$

where k_G is permeability of the materials expressed in cm/s, $C_G = 0.1$, x = 2, γ_w is the unit weight of water (kN/m^3), μ_w is the dynamic viscosity and is expressed in Pa.s, C_U is the coefficient of uniformity (-).

Chapuis and Aubertin (2003) also adapted Kozeny–Carman (KC) to estimate the hydraulic conductivity of tailings based on the concept of the equivalent diameter derived from the specific surface area of the solid grains, S_m (Chapuis and Aubertin 2003):

$$k = 10^{\left[0.5+\log\left(\frac{e^3}{D_R^2 S^2 (1+e)}\right)\right]} \tag{6}$$

where D_R is the specific weight of the material ($D_R = \rho_s/\rho_w$)(-).

Simulations using either power function (Eq. 3), KC and KCM morels were performed, and the

dissipation rate of PWP and evolution of the settlement of tailings were compared with measurements.

2.3.4 Implementation of Hydraulic Conductivity and Stiffness Changes in FLAC3D

Coupled analysis are conducted incrementally in FLAC3D: changes in PWP because of fluid flow and volumetric strain increments from mechanical loops are evaluated in the hydraulic loops. These changes in PWP are then passed to the mechanical loop to update effective stresses and then calculate failure (if any) and volumetric strain changes. The coupled process is implemented alternately in FLAC3D to update change in PWP and volumetric strain. The constitutive law that represents the relation between stress, strain and fluid pressure used in FLAC3D is as follows (Itasca 2021):

$$\frac{1}{M}\frac{\partial p}{\partial t} + \frac{n}{s}\frac{\partial s}{\partial t} = \frac{1}{s}\frac{\partial \zeta}{\partial t} - \alpha\frac{\partial \varepsilon}{\partial t} \tag{7}$$

where M: Biot's modulus (N/m^2); p: fluid pressure; n: porosity; s: degree of saturation; α: Biot coefficient; ζ: variation of fluid content; ε: mechanical volumetric strain.

The continuous update of tailings stiffness and hydraulic conductivity in the model followed the same approach (Fig. 4). The geometry of the domain was first created, and the boundary conditions were assigned. Then, the input parameters for the fluid phase (porosity, fluid bulk modulus, fluid tension, hydraulic conductivity, and degree of saturation) and solid phase (dry density, friction angle, cohesion, bulk modulus, and shear modulus) were assigned. The fluid flow calculation is first turned off to prevent any flow and thus porewater pressure change (Itasca

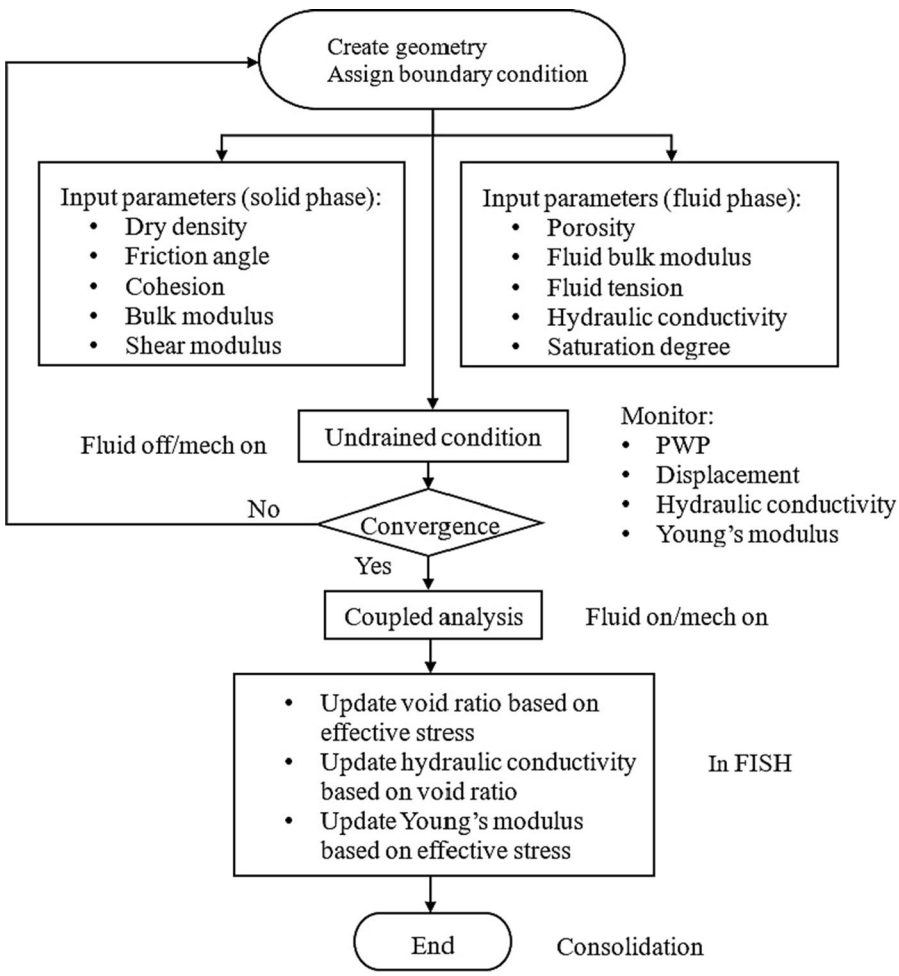

Fig. 4 Numerical approach to simulate tailings consolidation considering continuous update of stiffness and hydraulic conductivity

2021), and the model is iterated to reach mechanical equilibrium. This stage represents the moment where the loading is just applied to the material (i.e., undrained condition). However, this condition (fluid flow mode off) does not mean there is no excess porewater pressure within the materials, and in fact the excess porewater pressure is equal to the external loads (Itasca 2021). Once the model had converged, change in porewater pressure is allowed and it is converted into change in the effective stress by activating both fluid and mechanical loops in the model. Equations 2–6 were introduced in FLAC3D via FISH language (Supplementary materials). More specifically, the void ratio was calculated at every iteration based on the value of effective stress and was then used to automatically update the tailings hydraulic conductivity and stiffness. Finally, updated values of hydraulic conductivity and Young's modulus were assigned to the materials for the new iterations. The PWP, displacement, hydraulic conductivity and Young's modulus can be monitored during the modelling process.

2.3.5 Upscaling Models

To evaluate the continuous update approach under more realistic conditions, column test results were scaled up to simulate tailings consolidation behaviour in a typical tailings storage facility with sequential filling. In practice, tailings deposition rate widely varies depending on the production rate, TSF size and operational conditions at each mine site. For example, tailings filling rate is around 3 m/y at Malartic mine, Canada, (Bolduc and Aubertin 2014), and between 2 m/y and 14 m/y at Rabbit Lake mine, Canada (MEND 2015). In this study, a filling rate of 12 m per year was chosen as the base case, corresponding to the deposition of a 2-m thick layer every two months. A pseudo 3-D 12 m high model was simulated, with 0.5-m mesh. Bottom boundary was fixed, and side boundaries were only allowed to move vertically. The base of the model was considered impervious (bottom liner), and the water table was maintained at the surface of the model (as typically observed on slurry TSF during deposition). Tailings properties were the same as those in column test simulations.

Results on displacements and dissipation rate of PWP were compared with simulations considering constant stiffness and hydraulic conductivity. Details on the assigning values for the stiffness and hydraulic conductivity (i.e., continuously updated, updated at the beginning of each loading step or fixed values) are presented in Table 3.

3 Results

3.1 Column Test Simulations

Column test results showed that largest measured settlements occurred during the first few loading steps and the total measured settlements in columns S1 and S2 were around 3.15 and 3.44 cm, respectively, corresponding to around 10% of strain at the final loading steps (Fig. 5a, b). The total simulated settlement

Table 3 List of upscaling models in this study

Model	Properties		Specific features
	Hydraulic conductivity*	Stiffness	
M1	Updated	Updated	Continuously updated
M2	Updated	Fixed	E = 1800 kPa
M3	Updated	Fixed	E = 4500 kPa
M4	Updated	Updated	Young's modulus was only updated at the beginning of each loading step (instead of continuously in the previous cases), and hydraulic conductivity was continuously updated
M5	Fixed	Updated	$K_{sat} = 3.5 \times 10^{-7}$ m/s
M6	Fixed	Updated	$K_{sat} = 1.7 \times 10^{-7}$ m/s
M7	Fixed	Updated	$K_{sat} = 1.2 \times 10^{-7}$ m/s

*Update of hydraulic conductivity was continuous in all models where it was updated

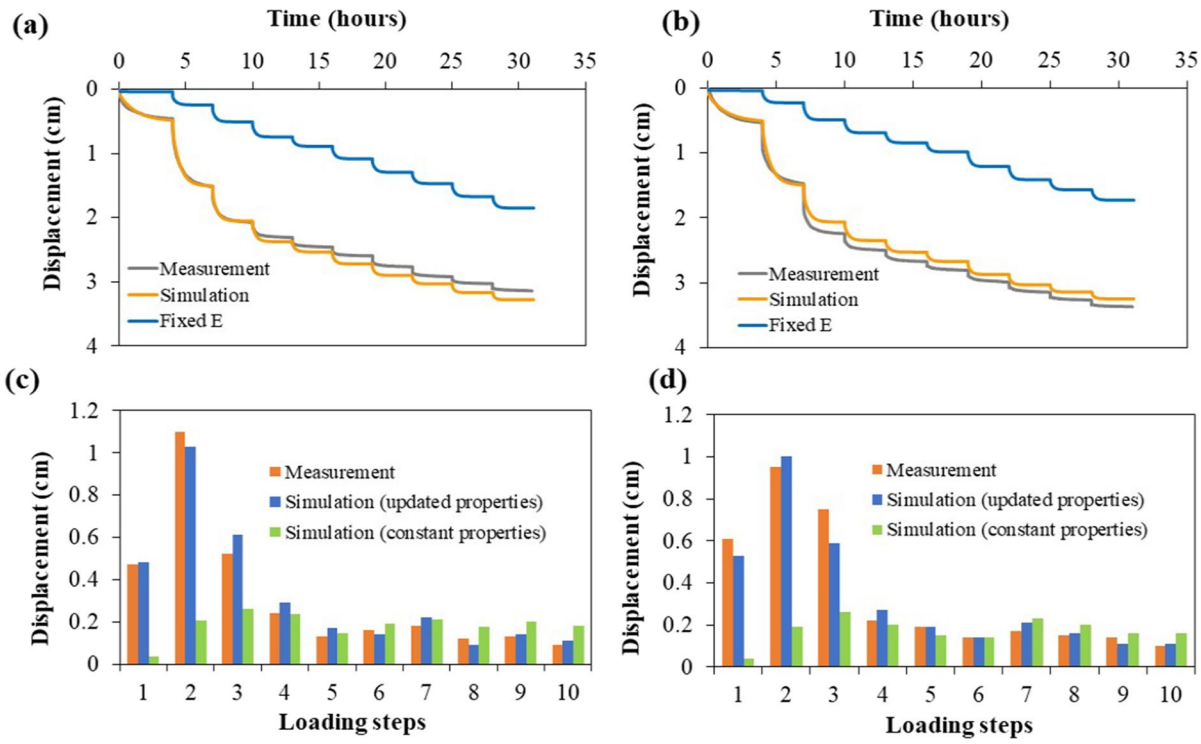

Fig. 5 Comparison of evolutions of simulated settlement with updated properties and measured settlement for the whole load cycles for **a** column S1, **b** column S2, and comparison of simulated (with updated and constant properties) settlements and measured settlement at each loading step for **c** column S1 and **d** column S2. Constant values of hydraulic conductivity (2.0×10^{-7} m/s) and stiffness (2500 kPa) corresponding to the intermediate values were assigned for tailings

in column S1 was 3.28 cm (4% greater than the measured value), and around 3.29 cm for column S2 (i.e., 4% lower than measured values) (Fig. 5a, b). The largest measured settlements occurred at the end of the 2nd loading step, with around 1 cm displacement for both columns (Fig. 5c, d). These might be attributed to the fact that the stiffness of tailings remained relatively low during the first few loading steps and that the increase of applied loads from the first to the second loadings step was significant (i.e., from 3.2 to around 22 kPa). Settlements then tended to decrease as loadings increased and the tailings became stiffer. For example, the measured settlement in column S1 was 0.52 cm during the 3rd cycle, and 0.1 cm during the last loading step (Fig. 5c). Simulated settlements showed a good agreement with measurements for all load cycles and for both columns (Fig. 5c, d). The difference between measured and simulated settlements was relatively small and usually below 15%. Maximum difference of around 33% (at the end of the 8th load cycles) and 24% (at the end of the 3rd load cycle) was observed in column S1 and S2, respectively (Fig. 5c, d). These good agreements between the simulations and the measurements showed the advantages of the developed approach that can simulate the evolution of stiffness of tailings.

Simulated displacements of model using a constant stiffness (E = 2500 kPa corresponding to the intermediate value) were significantly smaller compared to measured values (Fig. 5c, d). For example, simulated settlements at the end of the 2nd and 3rd load cycles in column S1 and S2 were around 5 and 3 times lower than measurements, respectively. The total simulated settlement in column S1 and S2 with constant stiffness was around 1.85 and 1.73 cm, respectively, which was approximately half of measured values. Results, therefore, confirmed that using a constant value for tailings stiffness may induce significant discrepancies compared to real tailings behaviour.

For each loading step, the excess PWP first increased to values corresponding to the loading applied and then gradually decreased towards

the hydrostatic pressure within usually around 1 h for both measured and simulated values (Fig. 6a). The evolution of simulated PWP in the middle of the columns matched relatively well measurements (Fig. 6a). For column S1, simulated t_{50} (time to achieve 50% of consolidation) and t_{90} (time to achieve 90% of consolidation) were generally greater than measured values. During the 3rd cycle, for example, around 10 min were required to dissipate 50% of excess PWP in column S1, but around double (i.e., 21 min) in the simulation, while simulated t_{90} was around 8 min higher than measured t_{90} during the 6th load cycle (Fig. 6a). The largest difference between measured and simulated t_{50} was at the end of the 2nd load cycle, with simulated t_{50} being 2.6 times longer than the measured value, while that of t_{90} was around 41% at the end of the 7th load cycle (Fig. 6b, c). These indicated that the models predicted relatively well the long-term dissipation of excess PWP compared to the short-term evolutions. The difference between measured and simulated t_{90} with constant hydraulic conductivity ($k = 2.0 \times 10^{-7}$ m/s) was around 40% with a maximum of 63% at the end of load cycle 9 (Fig. 6a). Similar trends were also observed for other load cycles and for the column S2. Simulations were therefore deemed acceptable considering usual uncertainties in displacement and hydraulic conductivity measurements.

Simulated evolutions of hydraulic conductivity and stiffness in column S1 were in a good agreement with measured values at each loading step (Fig. 7). In general, the difference between measured and simulated hydraulic conductivity was less than 10%. Saturated hydraulic conductivity exhibited a significant decrease after the first few layers, and the changes became smaller as loads increased. Saturated hydraulic conductivity was, for example, divided by two after the 2nd loading was applied, while the change was less than 10% after the application of the last few loads (Fig. 7a). Similar trends were observed for measured and simulated Young's modulus: a maximum difference of around 700 kPa (i.e., 20%) was observed at the last loading cycle, but in general, the difference between measured and simulated stiffnesses did not exceed 8% (Fig. 7b).

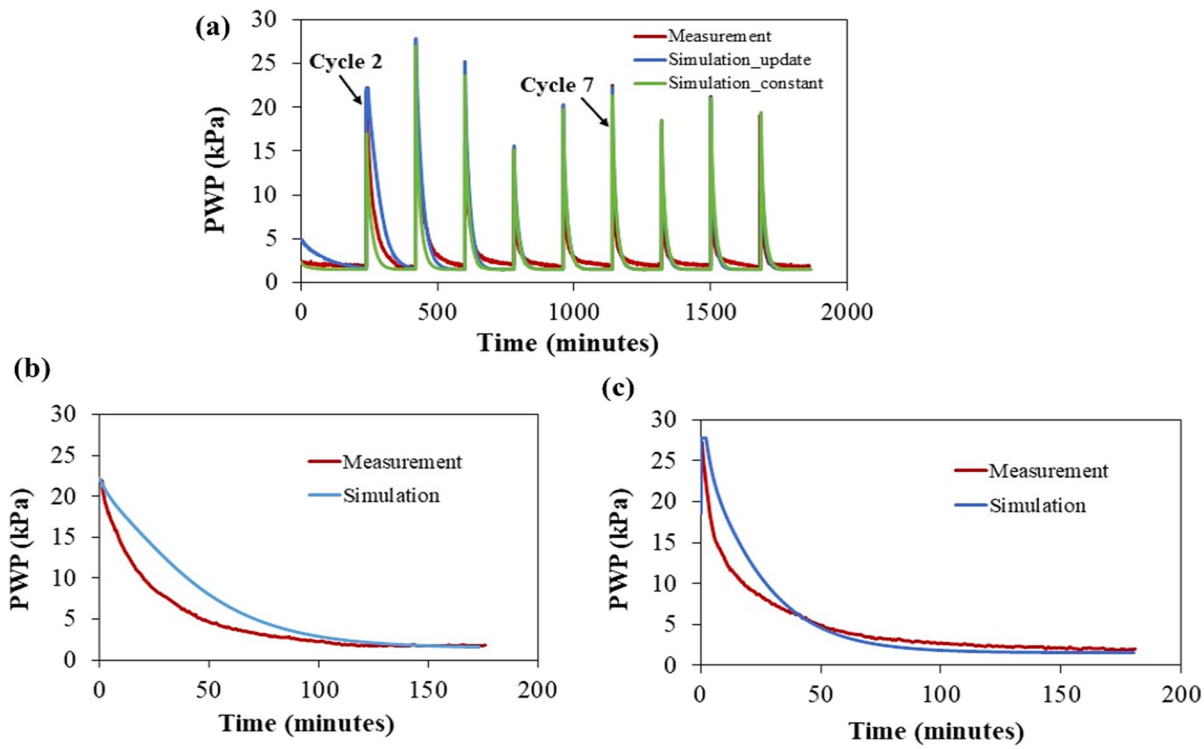

Fig. 6 Evolution of measured and simulated PWP in column S1 for **a** all load cycles, **b** the 2nd load cycle and **c** the 7th load cycle

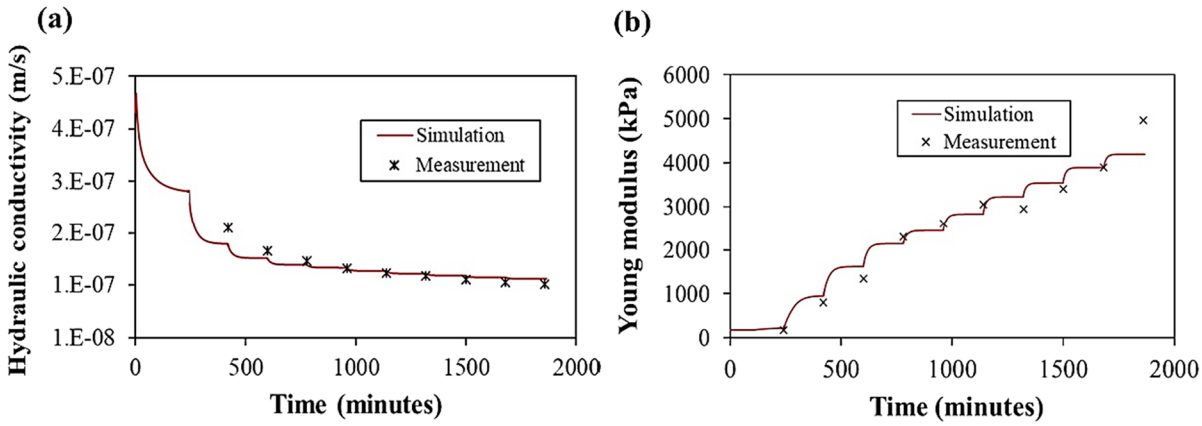

Fig. 7 Evolution of **a** tailings hydraulic conductivity and **b** Young's modulus in column S1 during column tests

Most of the changes between simulated and measured hydraulic conductivity and stiffness occurred during the first 30 min after the load was applied and then tended to become negligible.

3.2 Prediction of the Hydraulic Conductivity Function

Predictive models KCM and KC (Fig. 8) were used here to predict the hydraulic conductivity as a function of the void ratio of the studied tailings. Simulations using KCM and KC methods exhibited a faster dissipation rate of excess PWP compared to measured values. For example, around 20 min were required to dissipate 90% of excess PWP during the 3rd cycle with KC model, and 37 min with KCM, while measured t_{90} was around 61 min (Fig. 8a). A good agreement between results from KCM and KC models was observed at the beginning of the dissipation process (i.e., the difference between simulated and measured t_{50} was less than 20%). Similar trends were observed for the rate of settlements for all load cycles (Fig. 8b). Therefore, results indicated that predicting the hydraulic conductivity using KCM and KC models can provide acceptable results, at least, during the beginning of the dissipation process and can be used for a preliminary design stage. However, these predictive

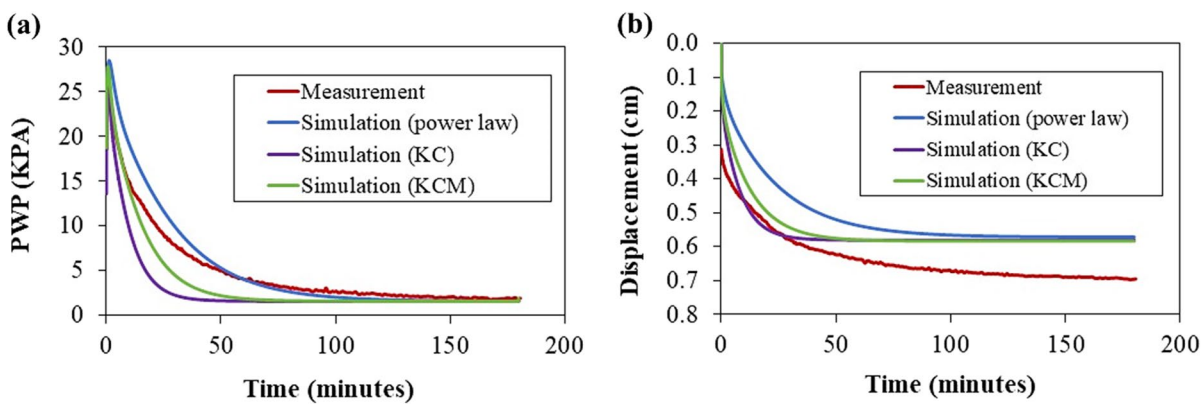

Fig. 8 Evolution of **a** excess PWP and **b** settlement with time during the 3rd loading step of column S2 for various estimation methods of hydraulic conductivity

functions tended to overestimate the dissipation rate of PWP in the long-term (t_{90} values) and measuring hydraulic conductivity is therefore recommended to improve the precision of the simulations.

3.3 Large Scale Implications

Large scale field models were simulated to evaluate the implications of using continuously updated hydraulic conductivity and stiffness to investigate tailings consolidation behaviour in the field. For the model with continuously updated properties, hydraulic conductivity decreased by around 2.5 times from 3.5×10^{-7} m/s at the beginning of filling process to 1.4×10^{-7} m/s after the filling of the last layer with a significant decrease occurring during the first 2 steps (Fig. 9a). On the contrary, Young's modulus increased tenfold during filling, reaching around 2500 kPa at the end of the filling process for the model where Young's modulus was updated (Fig. 9b). The model with continuously updated stiffness and hydraulic conductivity was then compared with simulations using a fixed value of Young's modulus or hydraulic conductivity (as frequently assumed in many literatures; see introduction). The consolidation behavior of the 6 layers was similar, and for conciseness, only results for the bottom layer are presented and interpreted here.

Simulations were first performed with fixed values of hydraulic conductivity ($k_{sat}=3.5\times10^{-7}$, 1.7×10^{-7} and 1.2×10^{-7} m/s) and continuously updated stiffness (model M5, M6 and M7). PWP first instantaneously increased by 40 kPa with the addition of each new 2-m thick tailings layer and subsequently dissipated until it reached hydrostatic conditions (Fig. 10a). The rates at which excess PWP dissipated were different for models with continuously updated or fixed values of hydraulic conductivity and the results may be overestimated and then underestimated (or the opposite) depending on the time the simulated hydraulic conductivity cross the constant values (Fig. 10). For example, after the 2nd layer was filled, the model with $k_{sat}=3.5\times10^{-7}$ m/s showed the fastest rate of PWP dissipation at the base of the tailings, with $t_{90}=4$ days, which was nearly half of that for a model with continuously updated hydraulic conductivity (Fig. 10b). Around 10.2 days were required to dissipate 90% of PWP when minimum hydraulic conductivity was assigned. t_{90} of model with continuously updated and intermediate hydraulic conductivity was essentially the same, which was around 7.8 days (Fig. 10b). After the addition of the sixth layer, the hydraulic conductivity of tailings at the bottom of the model was becoming smaller and close to its minimum value. Indeed, t_{90} for both models with minimum hydraulic conductivity and continuously updated hydraulic conductivity were close and around 35 days (Fig. 10c). t_{90} for model with maximum hydraulic conductivity was around 13.8 days, which was nearly 2.5 times faster compared to model with continuously updated conductivity (Fig. 10c).

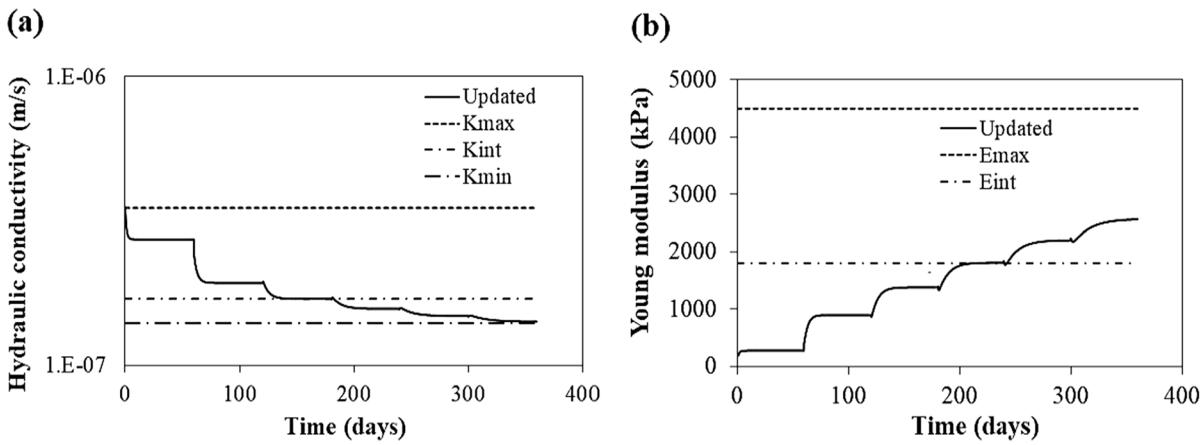

Fig. 9 Evolutions of **a** hydraulic conductivity and **b** Young's modulus of tailings at the middle of the first layer with time for models with continuously updated and fixed properties

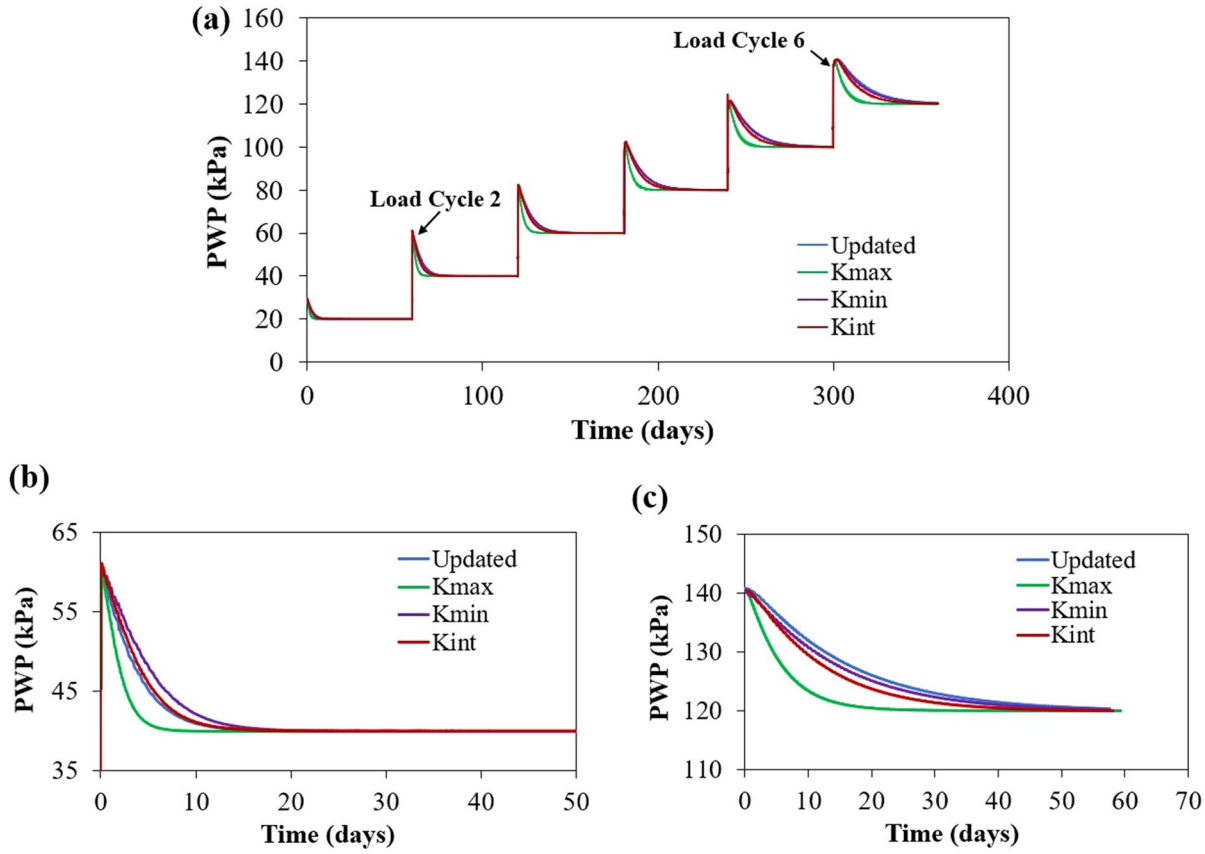

Fig. 10 Evolution of excess PWP at the base of the model **a** for the case of 2 m thick tailings layer, **b** after adding the 2nd layer and **c** after adding the 6th layer for models where hydraulic conductivity was continuously updated or fixed values were assigned

Models M2 and M3 with constant Young's modulus $E = 1800$ and 4500 kPa (derived from tailings properties in column tests) corresponding to the intermediate and maximum Young's modulus, respectively, were then performed (hydraulic conductivity was continuously updated continuously, see Table 3). Results showed that tailings settlements during sequential filling simulated with constant stiffness could lead to significant differences compared to those obtained with updated values. The model with maximum stiffness resulted in a settlement that was 5 times lower than that of a model with continuously updated stiffness at the end of the filling process (Fig. 11a). More specifically, the total settlement of the first layer for the model with continuously updated stiffness was around 15.7 cm, while those for models with maximum and intermediate values of Young's modulus were around 3.5 and 8.5 cm, respectively (Fig. 11a).

Another method to estimate the consolidation of tailings also consists of updating Young's modulus at the beginning of each loading step (corresponding to each new addition of a tailings layer) as mentioned previously. Model M4 was therefore simulated where Young's modulus was assigned a constant value at the beginning of each loading step was also performed (i.e., 180, 270, 890, 1390, 1800 and 2230 kPa corresponding to the loading step from 1 to 6). The settlement of the model with stiffness being updated at the beginning of each filling step was around 2.5 times higher than that of the model with continuously updated stiffness (Fig. 11a). The total settlement for the model of 6 layers and the total thickness of 12 m with Young's modulus being updated at the beginning of each filling stage was around 39 cm compared to 15.7 cm of the model with continuously updated stiffness (Fig. 11a).

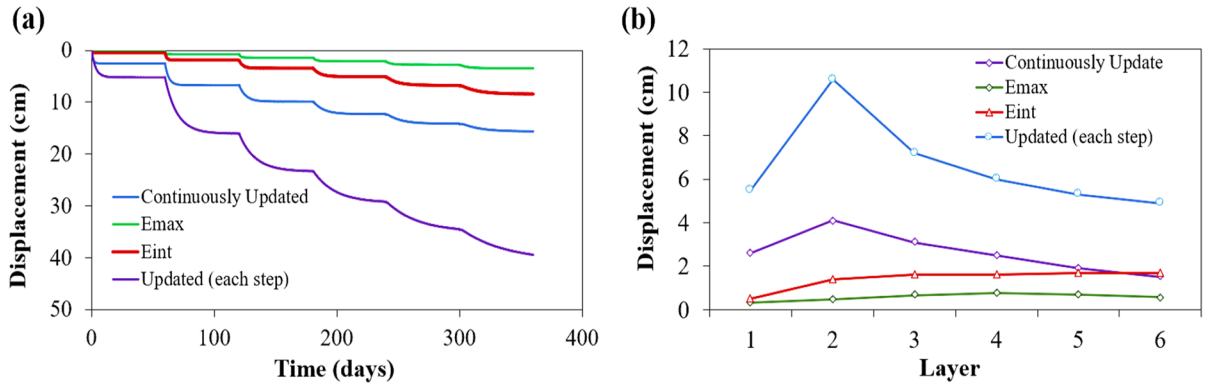

Fig. 11 Comparison of **a** evolution of the settlement of the bottom layer with time after filling of other layers in case of models with updated hydraulic conductivity and stiffness and models with fixed value of stiffness and **b** settlement of layer 1 resulting from the placement of other successive layers for these models

Also, the largest settlement of the first layer in continuously updated stiffness model occurred after the filling of the first two layers and the settlement then decreased as loading increased, while those of models with constant stiffness were relatively identical throughout the filling process (Fig. 11b). For example, the largest settlement of the first layer was around 4.1 cm after the addition of the second layer for the model with continuously updated stiffness and around 0.7 and 1.6 cm for almost all loading steps for models with maximum and intermediate stiffness, respectively (Fig. 11b). Continuously updated values could, therefore, contribute to improving the estimation of tailings settlement and, subsequently, of the volume of tailings that can be disposed of in the TSF in practice.

4 Discussion

The new approach proposed to automatically update stiffness and hydraulic conductivity seemed to improve simulation match with laboratory column test results. As a consequence, using a similar approach for field simulations may have a significant impact on the estimation of consolidation rate and magnitude of the tailings. It is therefore recommended to calibrate the equations representing evolutions of stiffness and hydraulic conductivity based on results from column tests. Being able to consider continuous change of saturated tailings properties can help to capture the evolution of excess PWP more precisely. This is crucial for the practical short-term design of TSFs, where it is necessary to calculate the filling rate of tailings to prevent the build-up of excess PWP, reducing the risk of TSFs failure (Rana et al. 2021; Fourie et al. 2022). The output results can also help to facilitate the estimation of volume of tailings that can be placed in TSFs, which is beneficial to the mine waste management operation in practice. However, despite the relatively good quality of the simulations, some limitations remained, mostly because of the necessary assumptions made.

More loading stages with smaller load increases should be added at the beginning of the column test at low pressures where most of the non-linear behaviour of tailings occur (Babaoglu and Simms 2020; Nguyen and Pabst 2020) to better capture the evolution of tailings at low values of load applied, which might be important in case the test is performed for the fine tailings (Fourie et al. 2022). Only 2 column tests were conducted in this study, and results are therefore limited to the tested tailings. Additional column tests and measurements of hydraulic conductivity are recommended to improve the precision of constitutive models of stiffness and hydraulic conductivity of tailings. For predictive functions, although both KCM and KC models can be used to estimate hydraulic conductivity of tailings at the preliminary design stage, care must be taken regarding the estimation of surface area while using KC model to improve the precision of the prediction (Chapuis and Aubertin 2003). Also, the shear strength will also change with the stiffness and hydraulic conductivity, but this was out of the scope

of this study which only focused on the consolidation evolution of the tailings.

Desaturation and desiccation at the top of tailings layers, which is frequent on TSFs, can also alter the rate of consolidation (Mbemba and Aubertin 2021b), but were not considered in this study. The approach developed however makes it possible to take these effects into account. Indeed, negative PWP can be applied at the top of the tailings in column test (Essayad and Aubertin 2021) to obtain relations for the evolution of tailings properties, which, in turn, can be numerically simulated.

Dilation angle was set as 0 in this study as recommended by Itasca (2021), yet the value of dilation angle may also influence the PWP evolution of the materials. More specifically, dilation angle would increase as the void ratio decreases during the shearing or consolidation of materials (Chakraborty and Salgado 2010) and the use of an associated flow rule along with the Mohr–Coulomb criterion would largely overestimate the material dilation (Itasca 2021). More studies on the influences of dilation angle on the PWP evolution should therefore be conducted.

Finally, results should also be compared with field measurements to confirm the extrapolability of the approach to real TSFs. Also, the simplified model and geometry of the TSF could influence the rate of consolidation. The effect of other factors such as the TSF geometry, configuration of drainage system or boundary conditions should also be evaluated.

5 Conclusions

This paper investigated the non-linear consolidation properties of saturated mine tailings under compression in a column test and a simplified large-scale model. A comprehensive study has been carried out to propose an approach to consider the non-linear behaviour of tailings in 3D analysis. The capability of the modified model was then successfully validated by modelling the column tests of saturated tailings. Later, the possibility to use predictive functions (namely KCM and KC models) to evaluate the *k-e* relation was investigated. Finally, the effect of using constant stiffness and hydraulic conductivity on settlement and PWP dissipation rate was studied. From this study, several conclusions can be drawn as follows.

The modified constitutive model was able to simulate the non-linear behaviour of tailings during the consolidation process with an acceptable accuracy. The total simulated settlement was 3.15 and 3.44 cm for column S1 and S2, respectively, which was fairly close to the measured values. The maximum difference between measured and simulated settlement during staged loading could reach up to 33%, while that for the rate of excess PWP was around 40%. Such differences were deemed acceptable considering typical uncertainty in displacement and hydraulic conductivity measurements in consolidation tests. The difference between simulated and measured hydraulic conductivity was less than 10% and 20% for stiffness values. Using constant properties can lead to a total settlement being around 2 times lower than measured values for column tests.

Model using KCM predictive model captured fairly well the evolution of excess PWP, while KC model tended to simulate a much faster dissipation rate than measured. KCM model seemed, therefore more suitable if tailings hydraulic conductivity was not measured in the lab.

Upscaling models indicated that the difference between models with constant and continuously updated tailings properties was significant. The excess PWP dissipation rate of tailings was 2.5 times faster when using a constant hydraulic conductivity compared to the model with updated hydraulic conductivity. The use of a constant value of stiffness could induce significant differences in the estimation of the settlement of tailings (i.e., up to 5 times of difference), while the settlement of models with stiffness being updated at the beginning of each filling step was around 2.5 times higher than that of the model with continuously updated stiffness. These indicated that the use of continuously updated values was more suitable when computing tailings consolidation behaviour, especially in the short term.

This study has shown the advantages of models with continuously updated values of stiffness and hydraulic conductivity of tailings. Further work should, however, be carried out to take into account the heterogeneous properties of tailings in the real TSFs and scale up to study the consolidation of tailings disposed of in an open pit.

Acknowledgements The authors are thankful to the financial support from NSERC, FRQNT and the partners of the Research Institute on Mines and the Environment (RIME UQAT—Polytechnique; http://rime-irme.ca/en). The authors also gratefully acknowledge Dr. Huy Tran, Dr. Kazim, Itasca technical support team for their valuable support and comments to improve the code in this study and Dr. Suman (University of Miami) for his comments to improve the manuscript.

Author contributions NDN: Performed the tests; conceived and designed the analysis; collected the data from literature; performed the numerical simulations; data curation; writing—original draft. TP: Conceived and designed the analysis; developed an approach for analysis of the results; supervision; writing—review and editing; funding acquisition.

Funding Open access funding provided by Norwegian Geotechnical Institute. Ngoc Dung Nguyen reports financial support was provided by Quebec Research Fund Nature and Technology.

Data Availability Enquiries about data availability should be directed to the authors.

Declarations

Conflict of interest The authors have no relevant financial or non-financial interests to disclose.

Open Access This article is licensed under a Creative Commons Attribution 4.0 International License, which permits use, sharing, adaptation, distribution and reproduction in any medium or format, as long as you give appropriate credit to the original author(s) and the source, provide a link to the Creative Commons licence, and indicate if changes were made. The images or other third party material in this article are included in the article's Creative Commons licence, unless indicated otherwise in a credit line to the material. If material is not included in the article's Creative Commons licence and your intended use is not permitted by statutory regulation or exceeds the permitted use, you will need to obtain permission directly from the copyright holder. To view a copy of this licence, visit http://creativecommons.org/licenses/by/4.0/.

References

Agapito LA, Bareither CA (2018) Application of a one-dimensional large-strain consolidation model to a full-scale tailings storage facility. Miner Eng 119:38–48. https://doi.org/10.1016/j.mineng.2018.01.013

Ahmed SI, Siddiqua S (2014) A review on consolidation behavior of tailings. Int J Geotech Eng 8:102–111. https://doi.org/10.1179/1939787913Y.0000000012

Ahmed M, Beier NA, Kaminsky H (2023) A comprehensive review of large strain consolidation testing for application in oil sands mine tailings. Mining 3:121–150

ASTM D1557-12 (2015) Standard test methods for laboratory compaction characteristics of soil using modified effort

ASTM D2487-17 (2017) Standard practice for classification of soils for engineering purposes (unified soil classification system)

ASTM D5856 (2015) Standard test method for measurement of hydraulic conductivity of porous material using a rigid-wall, compaction-mold permeameter: West Conshohocken Philadelphia

ASTM D6913/D6913M-17 (2017) Standard test methods for particle-size distribution (gradation) of soils using sieve analysis

ASTM D7928-17 (2017) Standard test method for particle-size distribution (gradation) of fine-grained soils using the sedimentation (hydrometer) analysis

Azam S, Li Q (2010) Tailings dam failures: a review of the last one hundred years. Geotech News 28:50–53

Azam S, Khaled SM, Kotzer T, Mittal HK (2014) Geotechnical performance of a uranium tailings containment facility at Key Lake, Saskatchewan. Int J Min Reclam Environ 28:103–117. https://doi.org/10.1080/17480930.2013.787702

Babaoglu Y, Simms P (2020) Improving hydraulic conductivity estimation for soft clayey soils, sediments, or tailings using predictors measured at high-void ratio. J Geotech Geoenviron Eng 146:6020016. https://doi.org/10.1061/(ASCE)GT.1943-5606.0002344

Bartholomeeusen G, Sills GC, Znidarčić D et al (2002) Sidere: numerical prediction of large-strain consolidation. Géotechnique 52:639–648. https://doi.org/10.1680/geot.2002.52.9.639

Bolduc F, Aubertin M (2014) Numerical investigation of the influence of waste rock inclusions on tailings consolidation. Can Geotech J 51:1021–1032. https://doi.org/10.1139/cgj-2013-0137

Boudrias G (2018) Évaluation numérique et expérimentale du drainage et de la consolidation de résidus miniers à proximité d'une inclusion de roches stériles. (Mémoire de maîtrise), École Polytechnique de Montréal

Bussière B (2007) Colloquium 2004: hydrogeotechnical properties of hard rock tailings from metal mines and emerging geoenvironmental disposal approaches. Can Geotech J 44:1019–1052. https://doi.org/10.1139/t07-040

Chai S, Zheng J, Li L (2023) Kink effect on the stress distribution in 2D backfilled stopes. Geotech Geol Eng 41:3225–3238. https://doi.org/10.1007/s10706-023-02434-4

Chakraborty T, Salgado R (2010) Dilatancy and shear strength of sand at low confining pressures. J Geotech Geoenviron Eng 136:527–532. https://doi.org/10.1061/(ASCE)GT.1943-5606.0000237

Chapuis RP, Aubertin M (2003) On the use of the Kozeny–Carman equation to predict the hydraulic conductivity of soils. Can Geotech J 40:616–628. https://doi.org/10.1139/t03-013

Da Silva MA, Lopes Motta F, Soares JBP (2021) Recovery of residual bitumen, dewatering, and consolidation of oil sands tailings with poly(acrylamide-co-lauric acid). Miner Eng 174:107248. https://doi.org/10.1016/j.mineng.2021.107248

Essayad K, Aubertin M (2021) Consolidation of hard rock tailings under positive and negative pore-water pressures:

testing procedures and experimental results. Can Geotech J 58:49–65. https://doi.org/10.1139/cgj-2019-0594
Essayad K (2015) Développement de protocoles expérimentaux pour caractériser la consolidation de résidus miniers saturés et non saturés à partir d'essais de compression en colonne. (Mémoire de maîtrise), École Polytechnique de Montréal
Ferdosi B, James M, Aubertin M (2015) Investigation of the effect of waste rock inclusions configuration on the seismic performance of a tailings impoundment. Geotech Geol Eng 33:1519–1537. https://doi.org/10.1007/s10706-015-9919-z
Fourie A, Ramon V, Annika B, et al (2022) Geotechnics of mine tailings: a 2022 State of the Art. In: the 20th ICSMGE-State of the Art and Invited Lectures. Sydney, Australia
Fredlund M, Donaldson M, Chaudhary K (2015) Pseudo 3-D deposition and large-strain consolidation modeling of tailings deep deposits. In: Tailings and mine waste. Vancouver, BC
Gheisari N, Qi S, Simms P (2023) Incorporation of three different creep models into large-strain consolidation analysis of a clayey tailings deposit. Comput Geotech 161:105533. https://doi.org/10.1016/j.compgeo.2023.105533
Gibson RE, England GL, Hussey MJL (1967) The theory of one-dimensional consolidation of saturated clays. Géotechnique 17:261–273. https://doi.org/10.1680/geot.1967.17.3.261
Holtz RD, Kovacs WD (1981) An introduction to geotechnical engineering. Prentice-Hall Inc, Englewood
Islam S, Williams DJ, Bhuyan MH (2023) Consolidation testing of tailings in a slurry consolidometer using constant rate and accelerated loading. Inst Civ Eng-Geotech Eng 176:295–305. https://doi.org/10.1680/jgeen.21.00065
Itasca (2021) FLAC3D 7.0 (Fast Lagrangian Analysis of Continua in 3 Dimensions) User Manual
James M, Aubertin M (2017) Comparison of numerical and analytical liquefaction analyses of tailings. Geotech Geol Eng 35:277–291. https://doi.org/10.1007/s10706-016-0103-x
Jeeravipoolvarn S, Chalaturnyk RJ, Scott JD (2008) Consolidation modeling of oil sands fine tailings: history matching. In: 61st Canadian Geotechnical Conference. Edmonton, Alberta, Canada, pp 190–197
Lévesque R (2019) Consolidation des résidus miniers dans les fosses en présence d'inclusions de roches stériles. (Mémoire de maîtrise), École Polytechnique de Montréal
Liu J, Znidarčić D (1991) Modeling one dimensional compression characteristics of soils. J Geotech Eng 117:162–169. https://doi.org/10.1061/(ASCE)0733-9410(1991)117:1(162)
Mbemba F, Aubertin M (2021a) Physical model testing and analysis of hard rock tailings consolidation considering the effect of a drainage inclusion. Geotech Geol Eng 39:2777–2798. https://doi.org/10.1007/s10706-020-01656-0
Mbemba F, Aubertin M (2021b) Physical and numerical modelling of drainage and consolidation of tailings near a vertical waste rock inclusion. Can Geotech J 58:1263–1276. https://doi.org/10.1139/cgj-2020-0372
Mbonimpa M, Aubertin M, Chapuis RP, Bussière B (2002) Practical pedotransfer functions for estimating the saturated hydraulic conductivity. Geotech Geol Eng 20:235–259. https://doi.org/10.1023/a:1016046214724
McDonald L, Lane JC (2010) Consolidation of in-pit tailings. In: Mine Waste 2010. Perth, Australia, pp 49–62
MEND (2015) MEND Report 2.36.1 In-pit disposal of reactive mine wastes: approaches, update and case study results
Morris PH (2002) Analytical solutions of linear finite-strain one-dimensional consolidation. J Geotech Geoenviron Eng 128:319–326. https://doi.org/10.1061/(ASCE)1090-0241(2002)128:4(319)
Ngo DH, Horpibulsuk S, Suddeepong A et al (2020) Consolidation behavior of dredged ultra-soft soil improved with prefabricated vertical drain at the Mae Moh mine, Thailand. Geotext Geomembr 48:561–571. https://doi.org/10.1016/j.geotexmem.2020.03.002
Nguyen D, Pabst T (2020) Comparative experimental study of consolidation properties of hard rock mine tailings. In: 73rd Canadian Geotechnical Conference (GeoVirtual 2020). Online
Nguyen ND, Pabst T (2023a) Consolidation behavior of various types of slurry tailings co-disposed with waste rock inclusions: a numerical study. Environ Earth Sci 82:65. https://doi.org/10.1007/s12665-023-10750-4
Nguyen ND, Pabst T (2023b) Acceleration of consolidation of tailings in a pit using waste rocks co-disposal. Geotech Geol Eng. https://doi.org/10.1007/s10706-023-02633-z
Nguyen ND (2022) 3D Numerical Evaluation of Consolidation of Tailings Co-Disposed with Waste Rocks in Open Pits (Ph.D.), Polytechnique Montréal, Retrieved from https://publications.polymtl.ca/10564/
Qiu YJ, Sego DC (2001) Laboratory properties of mine tailings. Canadian Geotech J 38:183–190. https://doi.org/10.7939/R3WW7704C
Rana NM, Ghahramani N, Evans SG et al (2021) Catastrophic mass flows resulting from tailings impoundment failures. Eng Geol 292:106262. https://doi.org/10.1016/j.enggeo.2021.106262
Schiffman RL (1982) The consolidation of soft marine sediments. Geo-Mar Lett 2:199–203. https://doi.org/10.1007/bf02462763
Somogyi F (1980) Large strain consolidation of fine grained slurries. In: Presentation at the Canadian Society for Civil Engineering. Winnipeg, Manitoba
Tian Z, Bareither C, Scalia J (2019) Development and assessment of a seepage-induced consolidation test apparatus
Townsend McVay (1990) SOA: large strain consolidation predictions. J Geotech Eng 116:222–243. https://doi.org/10.1061/(ASCE)0733-9410(1990)116:2(222)
Zhou, Amodio A, Boylan N (2019) Informed mine closure by multi-dimensional modelling of tailings deposition and consolidation. In: Mine Closure 2019. Perth, Australia

Publisher's Note Springer Nature remains neutral with regard to jurisdictional claims in published maps and institutional affiliations.